



Comparison of MGS TES FFSM eddies and MOC dust storms, MY 24–26

Integration of MY 26 eddies and dust storms



San José State
UNIVERSITY

John Noble^{1,2}, Robert M. Haberle², Alison F. C. Bridger^{1,2}, R. John Wilson³,
Jeffrey R. Barnes⁴, Jeffrey L. Hollingsworth², Melinda A. Kahre², Bruce Cantor⁵

1. San Jose State University, 2. NASA/Ames Research Center, 3. NOAA Geophysical
Fluid Dynamics Laboratory, 4. Oregon State University, 5. Malin Space Science Systems

Introduction

Mars Global Surveyor (MGS) orbiter observed a planet-encircling dust storm (PDS) in Mars year (MY) 25 from $L_s=176.2-263.4^\circ$ (Strausberg 2005; Cantor 2007). We have integrated and examined MGS data in order to better understand and characterize the dynamical processes responsible for MY 25 PDS initiation and expansion (Haberle *et al.* 2005; Noble *et al.* 2006, 2010, 2012; Wilson *et al.* 2008; Noble 2013). Here we integrate MY 26 Mars Orbiter Camera (MOC) visible dust storms and transient baroclinic eddies identified from Fast Fourier Synoptic Mapping (FFSM) of Thermal Emission Spectrometer (TES) temperatures and compare these with MY 24 & 25 data.

Uncertainty remains regarding PDS interannual variability. Are PDSs periodic or aperiodic, i.e. chaotic: governed by highly nonlinear, stochastically forced systems (Zurek and Haberle 1988)? Ingersoll and Lyons (1993) state that PDSs do not seem to be periodic, though statistics are limited. If PDSs are periodic, what environmental causes and dynamical mechanisms are responsible?

Datasets

- Thermal Emission Spectrometer (TES) measurements of atmospheric temperature and $9\text{-}\mu\text{m}$ dust opacity (Smith *et al.* 2001)
- Mars Orbiter Camera (MOC) daily global maps (DGM) produced by Malin Space Science Systems (Cantor 2007).
- Fast Fourier Synoptic Mapping (FFSM) of TES temperatures. FFSM is a spectral analysis method that creates synoptic maps from asynchronous data, maintaining full space-time resolution without distorting or smoothing higher frequency ($\sim 1-3$ sols) weather signals (Barnes 2001, 2003, 2006). This process removes the time mean, zonal mean, and westward diurnal tide.

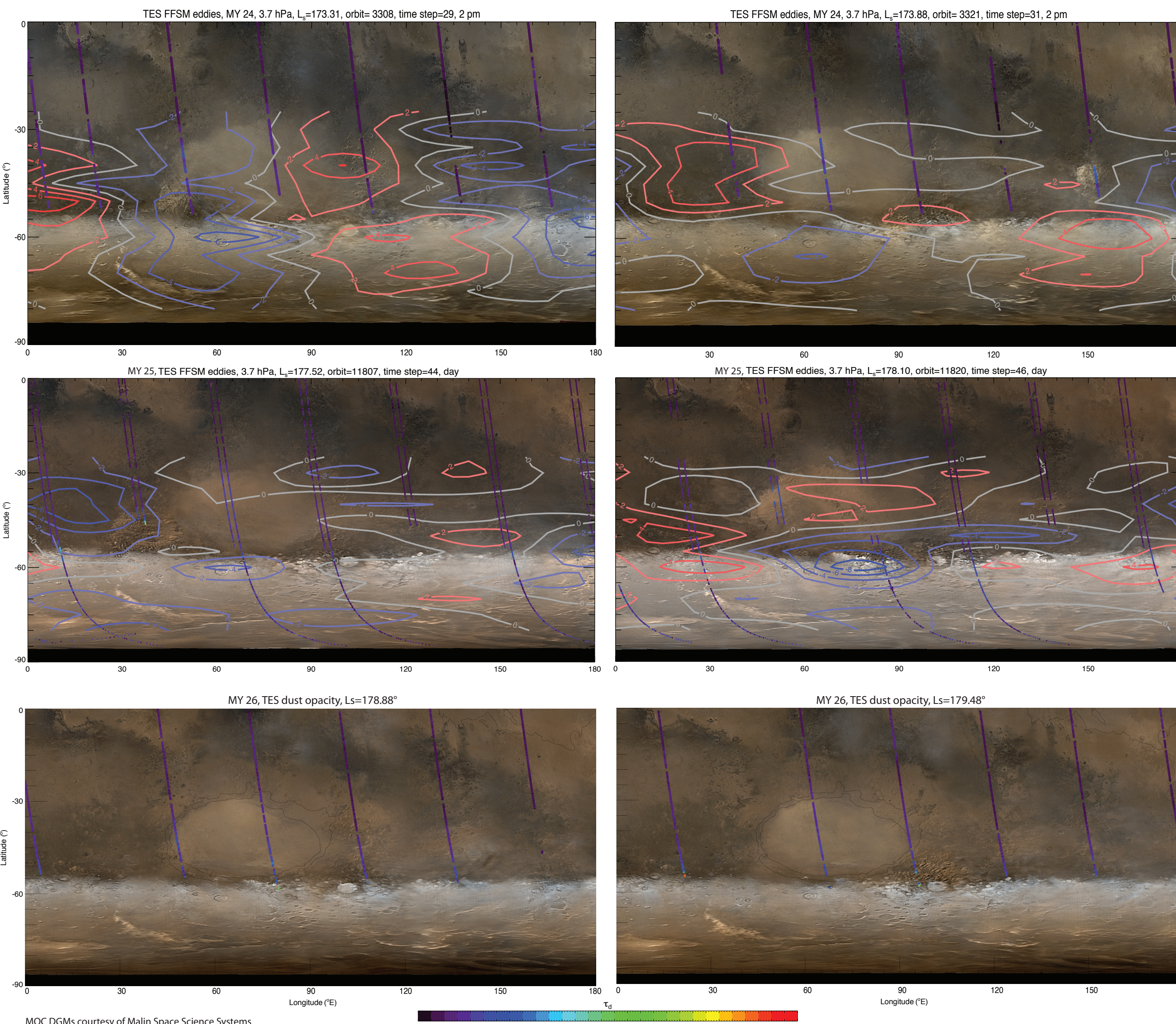
Objectives

The objectives of this work are to better understand and characterize the dynamical processes responsible for PDS initiation and expansion, specifically examining the following questions:

- Which circulation components were involved in storm onset and evolution?
- How did the temperature and dust opacity fields evolve together?
- Do MGS data show interannual variability that suggests why a PDS formed in MY 25 and not in MY 24 or 26?

Similarities, MY 24 – 26

- Concurrent eastward propagation of eddies and dust storms during this season
- Global phase speeds and periodicities (Table 1)
- Eastward and northward progression of dust storms through Hellas



Similarities, MY 24 – 26

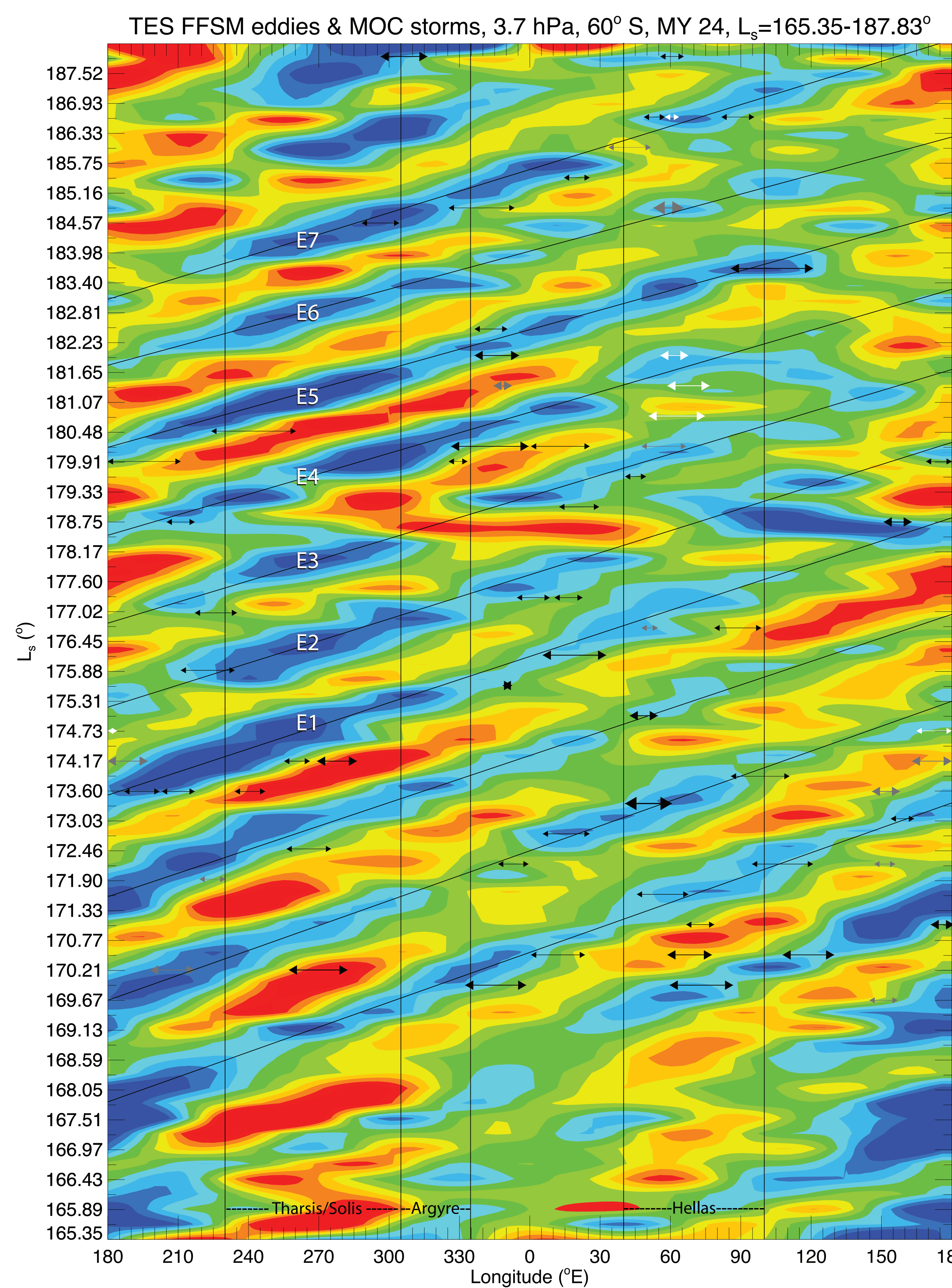
Eddy and dust storm propagation in Hellas (2 or 3-sol pattern)

- Eastward-travelling eddy (cold anomaly) reaches SW Hellas. Cap-edge dust storm(s) appears in SW Hellas (on eastern edge of cold anomaly)
- Eddy propagates into south-central Hellas ($60-80^\circ\text{E}$, $50-55^\circ\text{S}$) triggering additional cap-edge storms. Dust storm activity may appear in central Hellas ($\sim 40^\circ\text{S}$)
- Eddy travels to eastern Hellas. Dust storms are visible in mid ($35-45^\circ\text{S}$) to low ($25-35^\circ\text{S}$) latitudes in central Hellas. Cap-edge dust storms are visible in SE Hellas

MY 24: $L_s=172.75-173.88^\circ$;
MY 25: $L_s=175.80-176.37^\circ$; $L_s=177.52-178.10^\circ$; $L_s=182.15-183.32^\circ$; (Eddies 1, 2, & 5)
MY 26: $L_s=177.15-177.72^\circ$; $L_s=178.88-179.45^\circ$; $L_s=188.83-189.43^\circ$

L_s ($^\circ$) eddy at 60°E	Eddy #	c (m/s) global MY 24	c (m/s) global MY 25	c (m/s) global MY 26	P (sols) Hellas MY 24	P (sols) Hellas MY 25	P (sols) Hellas MY 26
176.5	E1	12.8	13.8				
178.0	E2	13.4	14.5	15.6	2.7	2.8	
179.3	E3	14.1	14.8	14.3	2.6	2.5	2.8
181.0	E4	14.5	13.1	13.8	2.8	3.0	2.9
182.7	E5	15.2	13.5		2.7	2.9	
184.6	E6	16.0	13.8	12.9	2.5	2.8	
186.3	E7	13.8	13.2	11.8	2.9	3.3	3.7
	Mean:	14.3	13.8	13.7	2.7	2.9	3.1

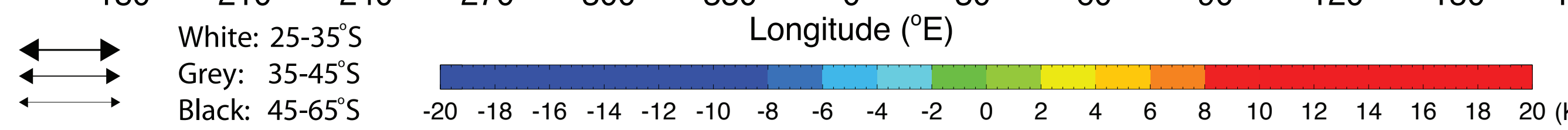
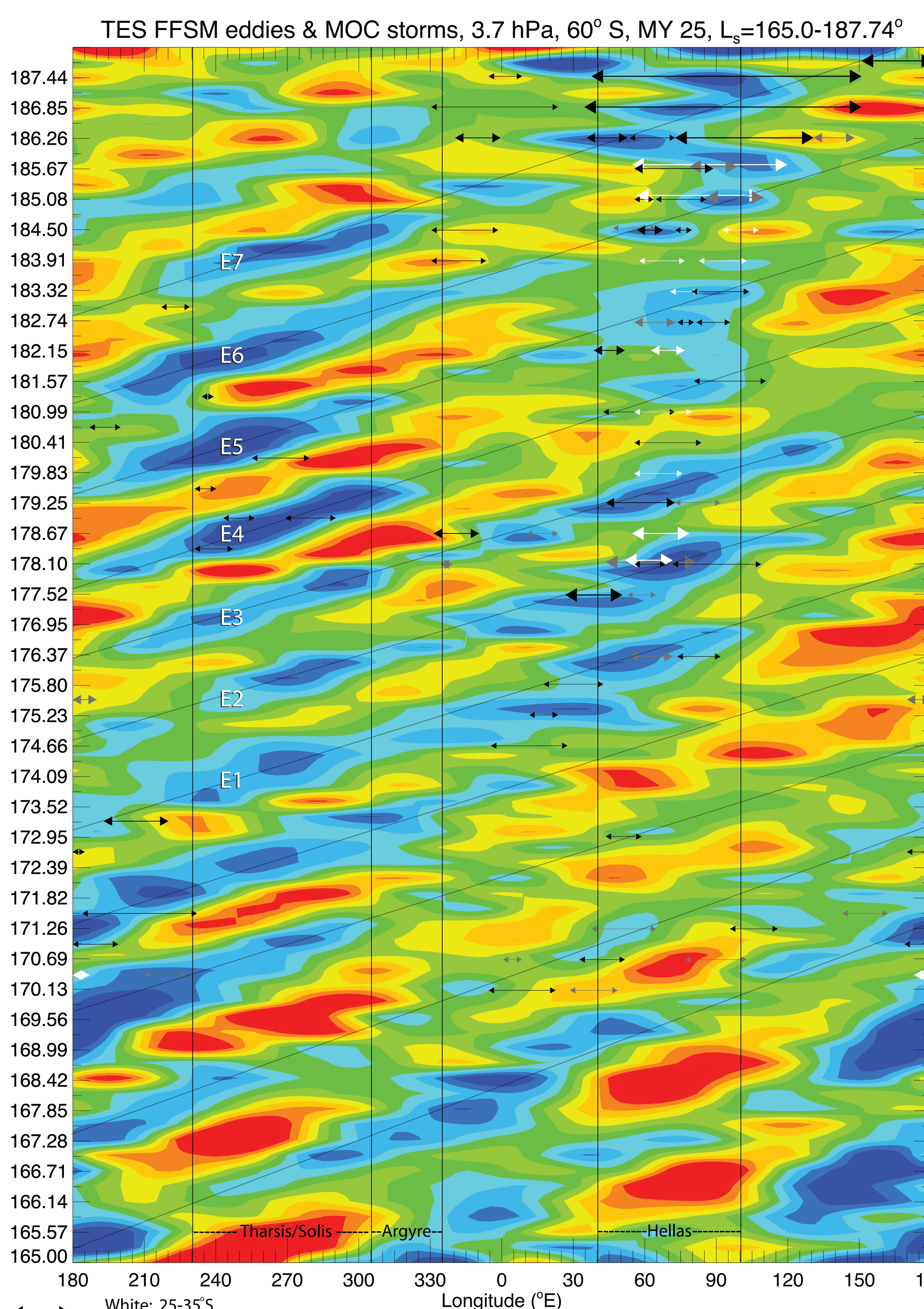
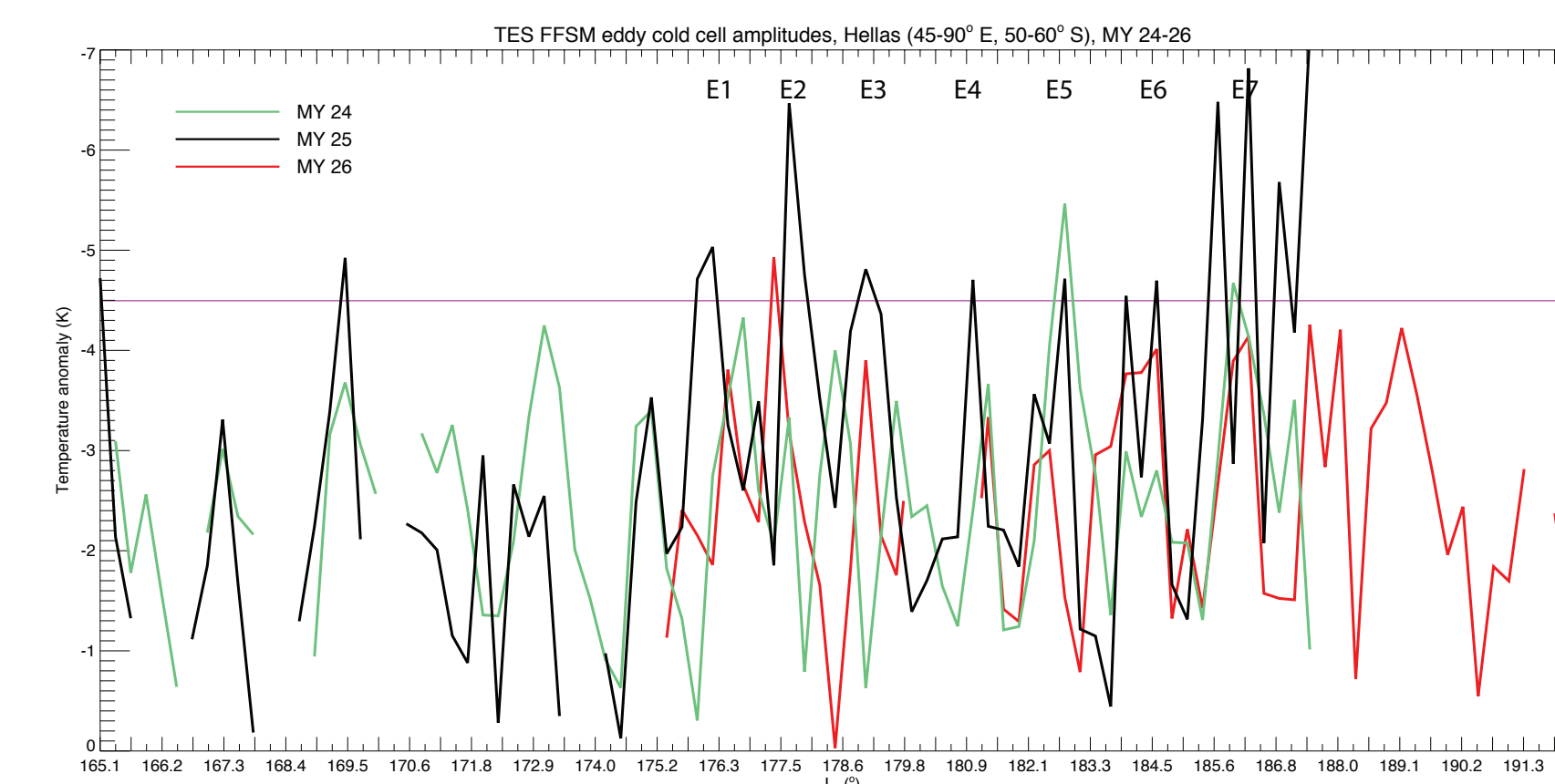
Table 1. TES FFSM eddy phase speeds, c, and period, P, at 60°E , MY 24–26



Arrows delimit the longitudinal extent of dust storms based on our analysis of MOC images. Three arrow sizes represent a subjective magnitude scale of apparent convective activity/structure, while colors represent storm central latitudes.

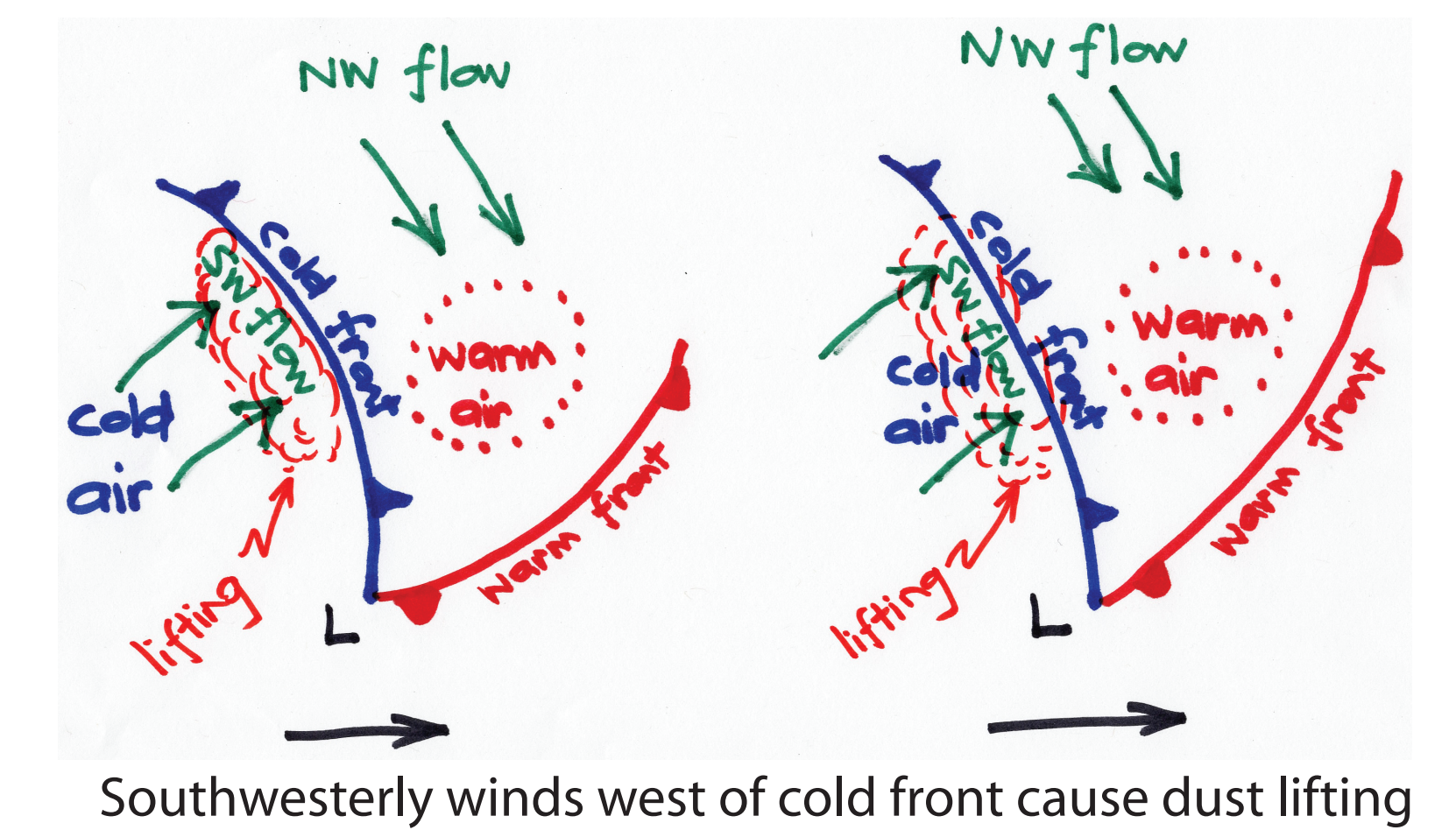
Differences, MY 24 – 26

- No large magnitude dust storms (τ_d or visual interpretation) observed in SW Hellas in MY 26 (c.f. MY 24, $L_s=173.33^\circ$ & MY 25, $L_s=177.59^\circ$)
- Different seasonal regime in MY 26 compared with MY 24 and 25. Cold centers appear to dominate the $90-220^\circ\text{E}$ longitude corridor from $L_s=175-183^\circ$, followed by a polarity switch to warm centers from $L_s=183-192^\circ$.
- Cold anomaly amplitudes:
 - MY 24: 2 eddies colder than -4.5K
 - MY 25: 7 eddies colder than -4.5K
 - MY 26: 1 eddy colder than -4.5K

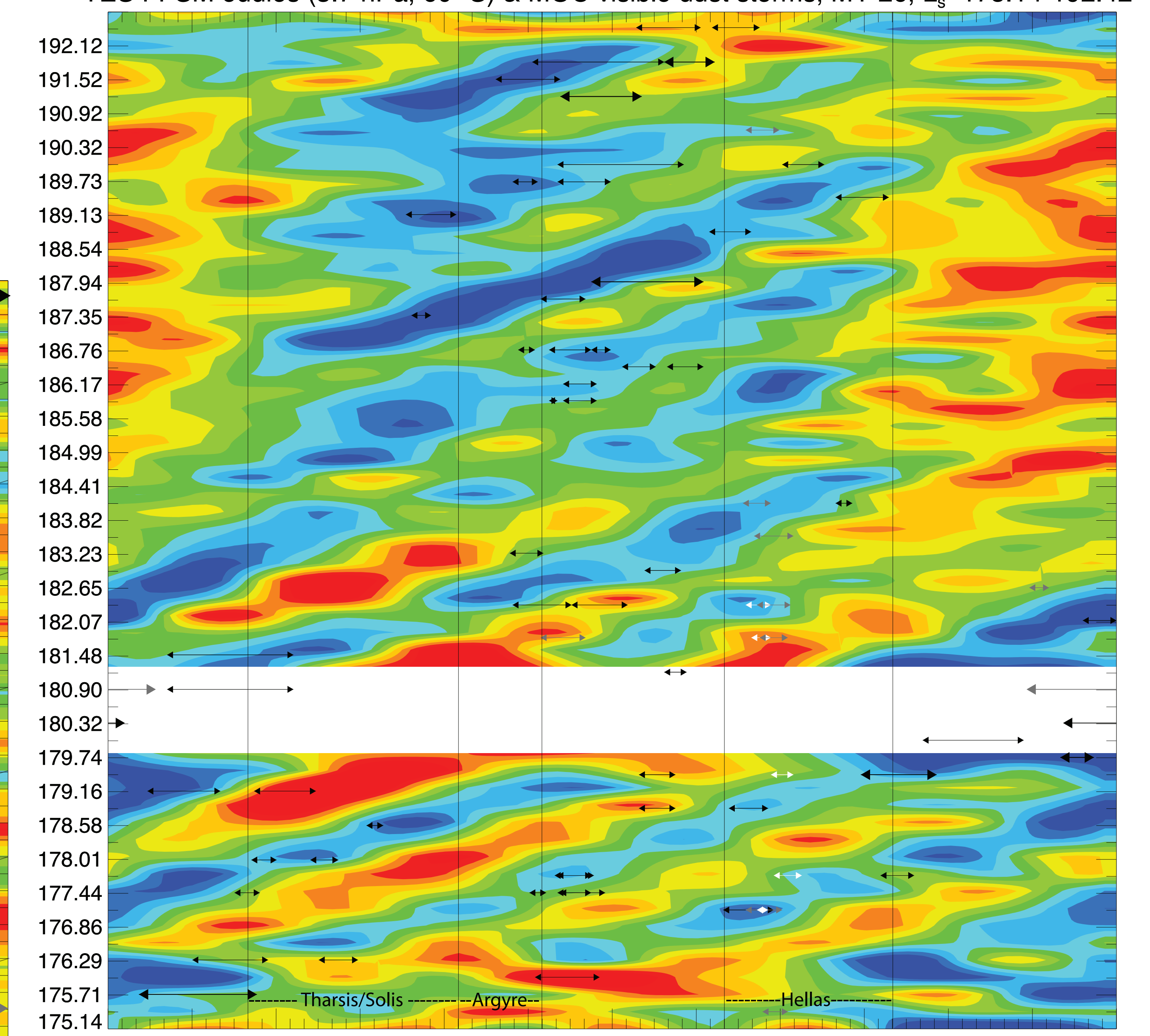


Southern hemisphere cold fronts and winds

Northward storm evolution is due in part to northward winds associated with cold fronts. Cold fronts are a characteristic of baroclinic eddies, and in the SH, baroclinic eddies cause northward winds.



TES FFSM eddies (3.7 hPa, 60° S) & MOC visible dust storms, MY 26, $L_s=175.14-192.42^\circ$



Working Hypothesis

- MY 25 PDS
- Six eastward-traveling baroclinic eddies (E1-E6) triggered the precursor storms due to the enhanced dust lifting associated with their low-level wind and stress fields.
 - Eddy E7 contributed to storm expansion on $L_s=186.3$
 - The sustained series of high-amplitude eddies in MY 25 was a factor in PDS occurrence that year.
 - Increased opacity and temperatures from dust lifting associated with eddies E1 – E3 enhanced thermal tides which supported further storm initiation and expansion out of Hellas.
 - Constructive interference of eddies and other circulation components may have led to the initiation and expansion of precursor storms. These include: CO_2 sublimation flow, anabatic winds, diurnal tides, and dust-induced thermal tides. Constructive interference increases surface stresses capable of lifting dust (through the wind field)
 - Non-dynamical factors in PDS interannual variability include dust sources and sinks

References

- Available on request